UNCLASSIFIED

AD NUMBER
AD224410
CLASSIFICATION CHANGES
TO: **UNCLASSIFIED**
FROM: **CONFIDENTIAL**
LIMITATION CHANGES
TO: **Approved for public release; distribution is unlimited.**
FROM: **Distribution authorized to U.S. Gov't. agencies and their contractors; Administrative/Operational Use; 15 APR 1952. Other requests shall be referred to Department of the Navy, Attn: Public Affairs Office, Washington, DC 20350.**
AUTHORITY
CNA ltr 4 Aug 1960 ; CNA ltr 4 Aug 1960

THIS PAGE IS UNCLASSIFIED

(1,0) [illegible]

UNCLASSIFIED

CONFIDENTIAL
[illegible] INFORMATION

22412

[illegible] GROUP
[illegible]
[illegible])

[illegible] REPORT[illegible]:
[illegible]
[illegible])

[illegible] of the Operations Evaluation [illegible] and is for information [illegible] reflect the official opinion [illegible] Operations. It includes information [illegible] rather than a technical nature [illegible] available only to those authorized [illegible].

[illegible] of this document in any form by other than [illegible] is not authorized except by special approval of [illegible] Naval Operations.

This [illegible] information affecting the [illegible] of the United States [illegible] of the Espionage Laws, [illegible] sections 793 and 794, the [illegible] of which in any manner [illegible] unauthorized person is prohibited by law.

Classification changed to **UNCLASSIFIED**

By authority of [illegible] 519 PC3EG of 4 Aug 1966

By

[illegible]
[illegible] RESEARCH GROUP
[illegible] Naval Operations

UNCLASSIFIED

CONFIDENTIAL
[illegible] INFORMATION

UNCLASSIFIED

B

UNCLASSIFIED

[illegible] operatic [illegible] for your info[illegible]

[illegible] publ [illegible] been

[illegible] numerous

[illegible] operations

[illegible]

Classification changed to [illegible]

By authority of CNO Ser [illegible] of [illegible]

By [illegible]

UNCLASSIFIED

771

04

CONFIDENTIAL
SECURITY INFORMATION

Op374/mjg
Ser 017P03D
5 Aug 1952

6. This material contains information affecting the national defense of the United States within the meaning of the Espionage Laws, Title 18, Sections 793 and 794, the transmission or revelation of which in any manner to an unauthorized person is prohibited by law.

DISTRIBUTION:
Attached list

[illegible] COPIES
[illegible] distribution

[illegible]ICATED

PAR[illegible]
[illegible] USN

(LO) [illegible]
1[illegible] A[illegible]

OPERATIONS EVALUATION GROUP
STUDY NO. [illegible]
([illegible])

VISUAL DETECTION IN AIR INTERCEPTION:
COMPARISON OF THEORY WITH TRIAL RESULTS
(Revised April [illegible])

ABSTRACT

Probabilities of detecting airplanes visually in daylight have been determined in trials conducted by the Naval Air Test Center, Patuxent River, Maryland. Comparison of the results with those predicted by visual-detection theory (OEG Study No. [illegible]) indicates that the theory adequately describes visual detection in air interception. The agreement between trial results and theory is better when the actual cross-sectional areas of the targets are used in computing the true ranges of detection than it is when the assumption is made that these ranges are proportional to the cube roots of the gross aircraft weights; but this approximation, suggested in Study No. [illegible], may be necessary when actual cross-sectional areas are unknown.

VISUAL DETECTION IN AIR INTERCEPTION: A COMPARISON OF THEORY WITH TRIAL RESULTS

(Revised April 1952)

Ref: (a) OEG Report 56 Search and Screening Conf 1946
(b) OEG Study No. 368 Visual Detection in Air Interception Conf 26 Oct 1946
(c) OEG Study No. 430 Addendum to OEG Study No. 368 Computation of Probability of Visual Detection in Air Interception Conf 21 Nov 1950
(d) OEG Study No. 371 The Problem of Visual and Radar Sighting in High-Speed, High-Altitude Interception Secret 3 Dec 1948
(e) CO-NAVAER OC-45RA-[illegible] Restr 1 Jan 1947
(f) CO-NAVAER Engineering Report No. DE-304 Characteristics Summary U.S. Navy Aircraft Secret 15 Oct 1948

I. INTRODUCTION

In spite of the improvements that have been made in other detection methods, visual sighting of enemy aircraft remains vital in air interception. C.I.C. information generally is insufficient to guide an aircraft into firing position. Consequently, final detection must often be by visual means.

Interest in visual detection was stimulated by the failure to sight Japanese Kamikaze attackers at ranges sufficient to defeat their mission and by the difficulties in conducting air-sea rescue operations. Attempts were made to obtain information on detection probabilities from detections of scale-model aircraft. These trials proved inconclusive, and no permament record of them was kept. Some experimental data on vision were available, however, and from them a basic theory of visual detection was constructed (reference (a)).

Reference (a) made special application of this theory to the sighting of surface ships from aircraft. Reference (b) applied this theory to the visual detection of airborne targets, and reference (c) presented a method that enabled one to calculate the probability of visual detection of a target aircraft by an airborne observer for a large number of conditions. Reference (d) undertook special treatment of

high-speed, high-altitude interception. But adequate experimental data by which to judge the theory were needed.

To furnish these data, a series of trials were conducted by the Naval Air Test Center, Patuxent River, Maryland, from 17 December [illegible] to 30 December [illegible]. These trials yielded [illegible] the probabilities of [illegible] under different operational conditions. [illegible] an investigation of the extent to which the visual-detection theory of reference ([illegible]) was verified in the trials.

A. [illegible]

[illegible]
(5)) [illegible]

[illegible] (1) and (2) [illegible] is de- [illegible] between target and [illegible] by the "[illegible] background [illegible] background [illegible] if the back[illegible] under day[illegible] in de- [illegible] difference (1) also [illegible] shape does not affect [illegible] that de[illegible] light are [illegible]

(1) [illegible]
(2) [illegible]

[illegible] characteristics of [illegible] is depe[illegible] the [illegible] the [illegible] image in [illegible] of the [illegible] dis[illegible] image from [illegible]

a function of the angular distance between the visual axis of the eye and the line joining the object with the eye.

B. DETECTION LOBE

Results of investigations by K.J.W. Craik are used in reference ([illegible]) and (b) to derive the following expression connecting brightness contrast C with range of target R, angle θ between the target and the visual axis, and area A of the cross section of the target in the plane perpendicular to the visual axis:

$$C = 1.75\theta^{\frac{1}{2}} + 45.6(\theta R^2)/A. \qquad (1)$$

Here R is in miles, A is in square feet, and θ is in degrees. (If θ is less than 0.8, this equation does not apply, and the value of R is the same as that determined for $\theta = 0.8$.) This equation defines a detection lobe, which can be thought of as a surface of revolution constructed about the eye's visual axis in such a manner that a target within the lobe can be seen and a target outside of the lobe cannot be seen. Actually, of course, visibility of an object is not that precisely determinable; some targets that fall within the detection lobe will be missed and others that fall outside of it will be detected. The lobe is drawn on the assumption that the number of targets detected is the same as though all that fall within the lobe are detected and all that fall outside it are missed.

C. HAZE

Haze in the atmosphere will reduce the apparent contrast of the target and thus reduce the range at which the target can be detected. Reference (a) connects intrinsic contrast C_0 with apparent contrast C by the expression

$$C = C_0 \exp(-3.44\ R/V), \qquad (2)$$

where V is the meteorological visibility or range at which large targets (such as mountains) can be seen. Substituting this into equation (1) gives

$$C_0 \exp(-3.44\ R/V) = 1.75\ \theta^{\frac{1}{2}} + 45.6(\theta R^2)/A. \qquad (3)$$

D. DETECTION RANGE

Maximum range of detection will be obtained when the target is imaged on the fovea. This will occur when θ is less than or equal to 0.5 degree, which is the approximate angular radius of the fovea. This substitution in equation (1) yields

$$R_m = 0.1655 \sqrt{(C-1.565)A} \qquad (4)$$

as an expression for maximum range R_m. The maximum range in the absence of haze, R_o, similarly becomes

$$R_o = 0.1655 \sqrt{(C_o - 1.565)A}. \qquad (5)$$

E. COMPUTATION OF DETECTION LOBE

Equations (3) and (5) connect visual perception angle θ with A, C_o, V, and R. If, instead of these, the variables R/R_o, R_o/V, and C_o are employed, the number of variables is reduced from 4 to 3. When this is done, the following expression is obtained for θ:

$$\theta = F \left\{ \sqrt{G/F + 1} - 1 \right\}^2 , \qquad (6)$$

where

$$F = 0.49 \, (R_o/R)^4 / (C_o - 1.565)^2$$

and

$$G = 0.80 \, C_o \exp(-3.44R/V)(R_o/R)^2 / (C_o - 1.565).$$

Details of a similar substitution involving R_m instead of R_o can be found in reference (a).

Equation (6) has been used in reference (b) to compute detection lobes for a wide variety of conditions. Two typical lobes are plotted in Figure 1. Curve A shows the

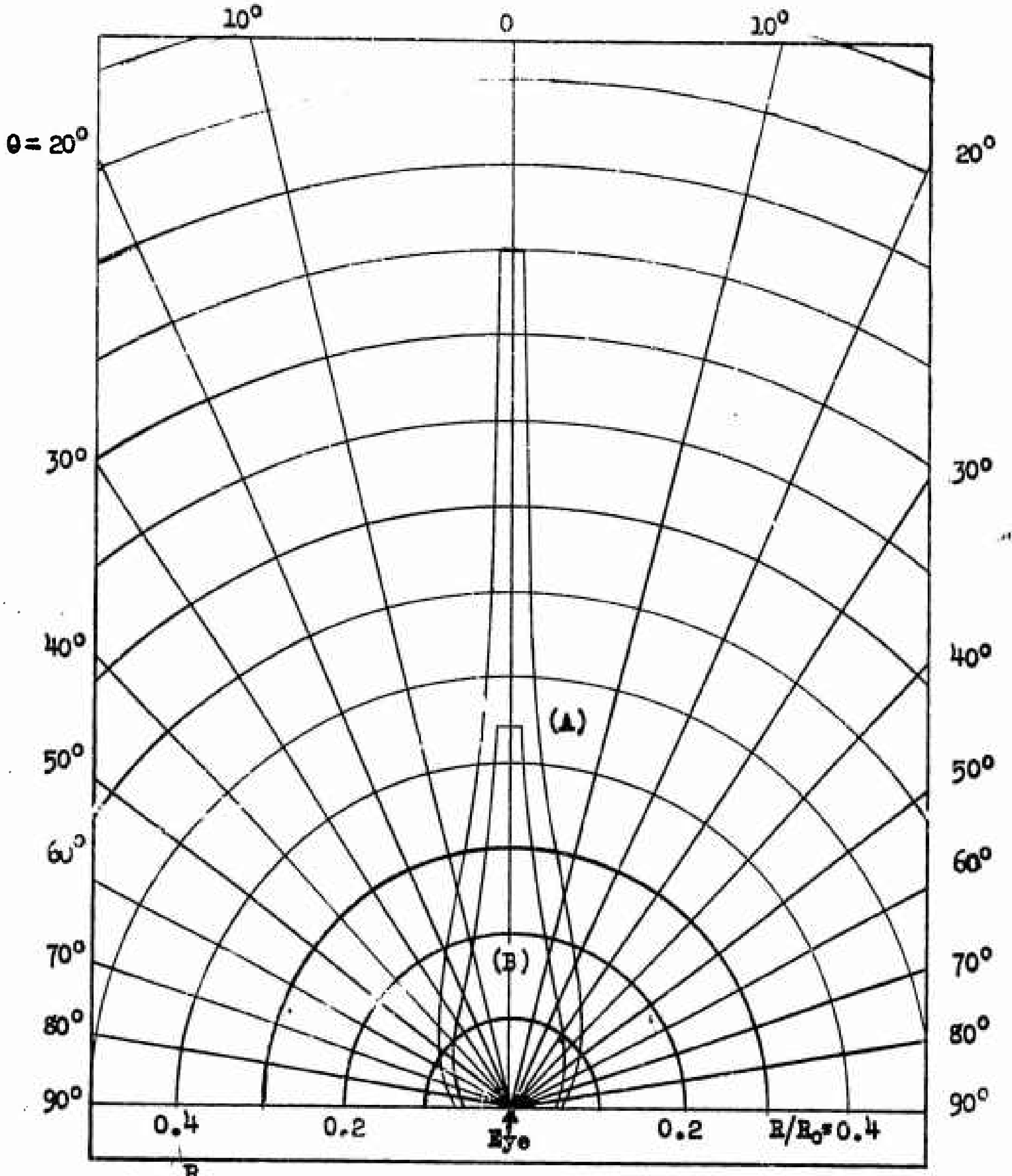

(A) $\frac{R_0}{V} = 0$

(B) $\frac{R_0}{V} = 1.0$

$C_0 = 50\%$

Range scale = R/R$_0$

Polar angle = θ

FIG. 1: TYPICAL DETECTION LOBES

Touc[illegible] under [illegible] shortening has [illegible] base, of th[illegible] coordi- so that [illegible]), [illegible] ted nate [illegible] second radi[illegible] will to [illegible] be de[illegible]

F. GLIMPSE PRO[illegible]

[illegible] to be appr[illegible]. When it is at [illegible] has ob- serve[illegible], it [illegible] that desc[illegible] (i) [illegible] this the e[illegible] poi[illegible] (7).

[illegible] to know something [illegible] ob- ject. The [illegible] a series [illegible]. If the [illegible] has no a[illegible] Ⓗ [illegible] the targe[illegible] de- expected [illegible] could continue [illegible] angle [illegible]:

$$[illegible] \qquad (7)$$

θ here is the angle [illegible] for the proper detection [illegible]). [illegible] may consist [illegible] is belie[illegible] ordinarily search[illegible]).

G. CUMULATIVE PRO[illegible] DE[illegible]

[illegible] undef- initely, [illegible] ant [illegible] target. itself [illegible]

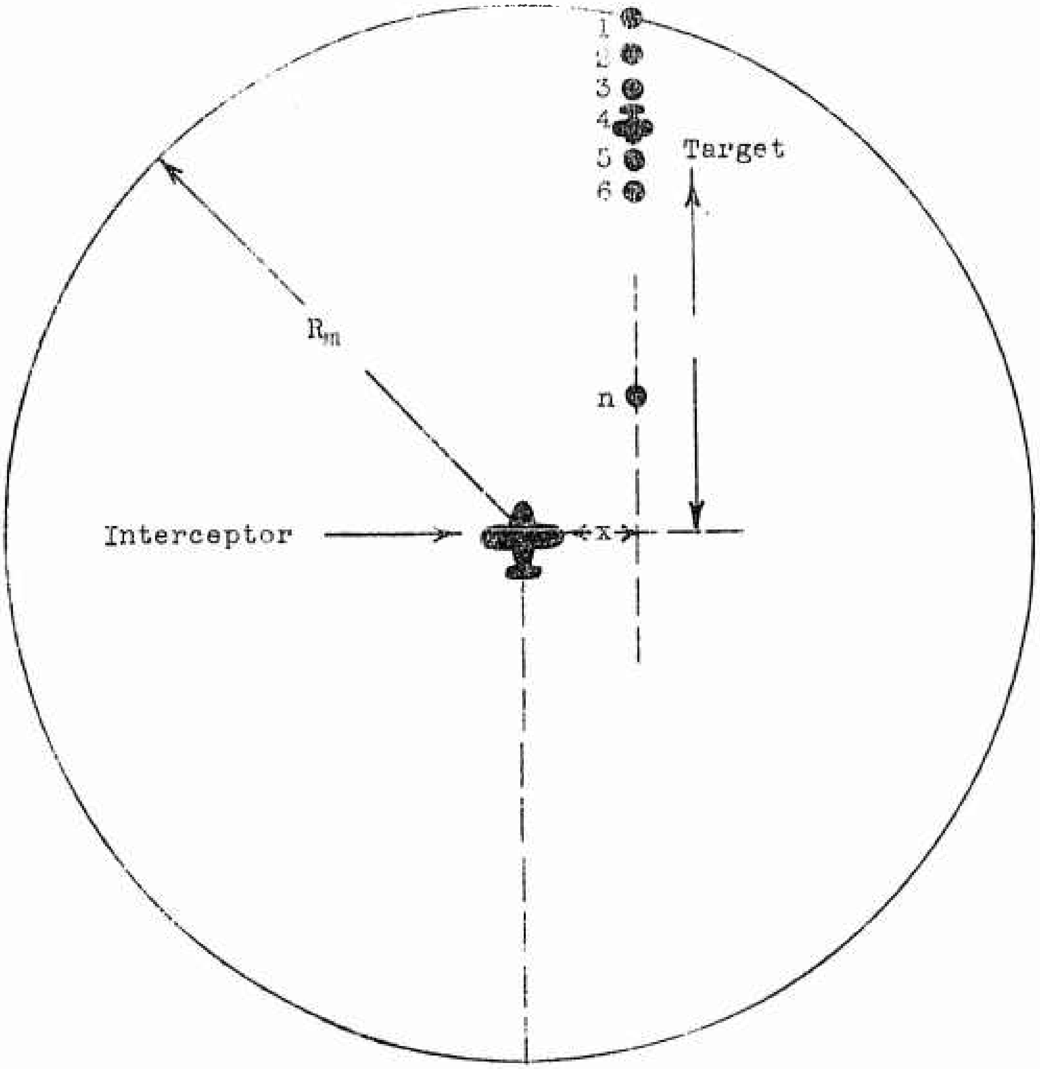

FIG. 2: GLIMPSE PROBABILITIES

The target, however, moves on to positions 2, 3, 4, --- n; so if it is not detected the instant it is at the extreme range, it will not be detected until it has reached some closer range. Let the probability that the target will be detected at position i be g_i. (See Equation (7).) Then the probability that it will not be detected at position (1) is $(1 - g_1)$, since the sum of the probability of successful detection and the probability of failure to detect must equal 1. The probability that the target will fail to be detected at all the positions 1, 2, 3, 4, ..., n is $(1 - g_1)(1 - g_2)(1 - g_3)(1 - g_4)\ldots(1 - g_n)$. Then the probability that the target will be seen initially at point n or earlier is

$$P_n = 1 - \prod_{1}^{n} (1 - g_i) \qquad (8)$$

where the symbol $\prod_{1}^{n}$ is used to indicate the product of the $(1 - g)$'s that were given in the preceding sentence, because the sum of the probabilities of initial successful detection at point n or earlier and the probability of failure to detect at any of the points up to and including point n is unity.

Equation (8) may be written in logarithmic form

$$P_n = 1 - \exp\left(\sum_{1}^{n} \ln(1 - g_i)\right) \qquad (9)$$

where $\exp(\sum_{1}^{n} \ln(1 - g_i))$ is the antilogarithm of the sum of the natural logarithms, and thus is equal to $\prod_{1}^{n} (1 - g_i)$.

Equations (8) and (9) give probabilities of detection for the particular target positions 1, 2, 3, ..., n. To obtain the average probabilities associated with all points on the target's course, the logarithm of each failure probability in (9) is converted to unit time by dividing by the average time between glimpses, T. The resulting failure

probability per unit time then is integrated over time to give

$$P_n = 1 - \exp\left[(1/T)\int_0^t \ln(1 - g_i)\,dt\right], \qquad (10)$$

which is more convenient if it is expressed in terms of distance

$$P_n = 1 - \exp\left[-(1/vT)\int_y^\infty \ln(1 - g_i)\,dy\right], \qquad (11)$$

where v is the relative velocity in knots.

For the special case in which the interceptor is on a collision course with the attacking aircraft, this equation reduces to

$$P = 1 - \exp(-R_o I/v) \qquad (12)$$

where I is the integral

$$I = \int_{R_2/R_o}^{R_1/R_o} 2.21\ (10^3)\ \ln(1 - g_i)\ d(R/R_o).$$

Here R_1 is the range at which search begins and R_2 is the range at which the interceptor has closed to obtain the probability of detection P. This special situation corresponds to the one existing during the trials. (See Section III).

H. METHOD OF DETERMINING PROBABILITY

From the formulas given in the preceding paragraphs, it is possible to determine the theoretical probability of detecting an air target if the necessary parameters are known.

Thus, if [illegible] contrast C_0 are known, the range R_0 [illegible] determined from equation (1). [illegible] θ [illegible] the visual axis at which [illegible] by the eye can be determined from [illegible] is [illegible]. [illegible]

(11) [illegible]

I. DETE[illegible]

[illegible] shape of the airplane [illegible] with the visual axis [illegible] Aircraft [illegible] specifications, [illegible] preceding paragraph is not always [illegible]. To permit the determination of R_0 in [illegible] available characteristic of the airplane, [illegible] (5) suggests that the maximum range [illegible] a linear dimension of the aircraft, [illegible] proportional to the cube root of the [illegible], Figure 3, which is taken from reference (5), [illegible] of the cube root of the gross [illegible] contrast C_0. A typical set of [illegible] using this [illegible] and giving range [illegible] aspect angle for different probabilities [illegible].

Thus [illegible] probability that [illegible]. One [illegible] target area A, deter[illegible], to determ[illegible]. The [illegible] the [illegible] the cube [illegible]. [illegible] method hence[illegible] forth [illegible], since it follows directly from [illegible]. [illegible] be termed the approximat[illegible].

In [illegible] attack angle [illegible] is assumed [illegible] the bow [illegible] cross-[illegible]. [illegible] method, [illegible] formulas for [illegible] α [illegible] range at [illegible] angle α [illegible], are given in Section II-D.

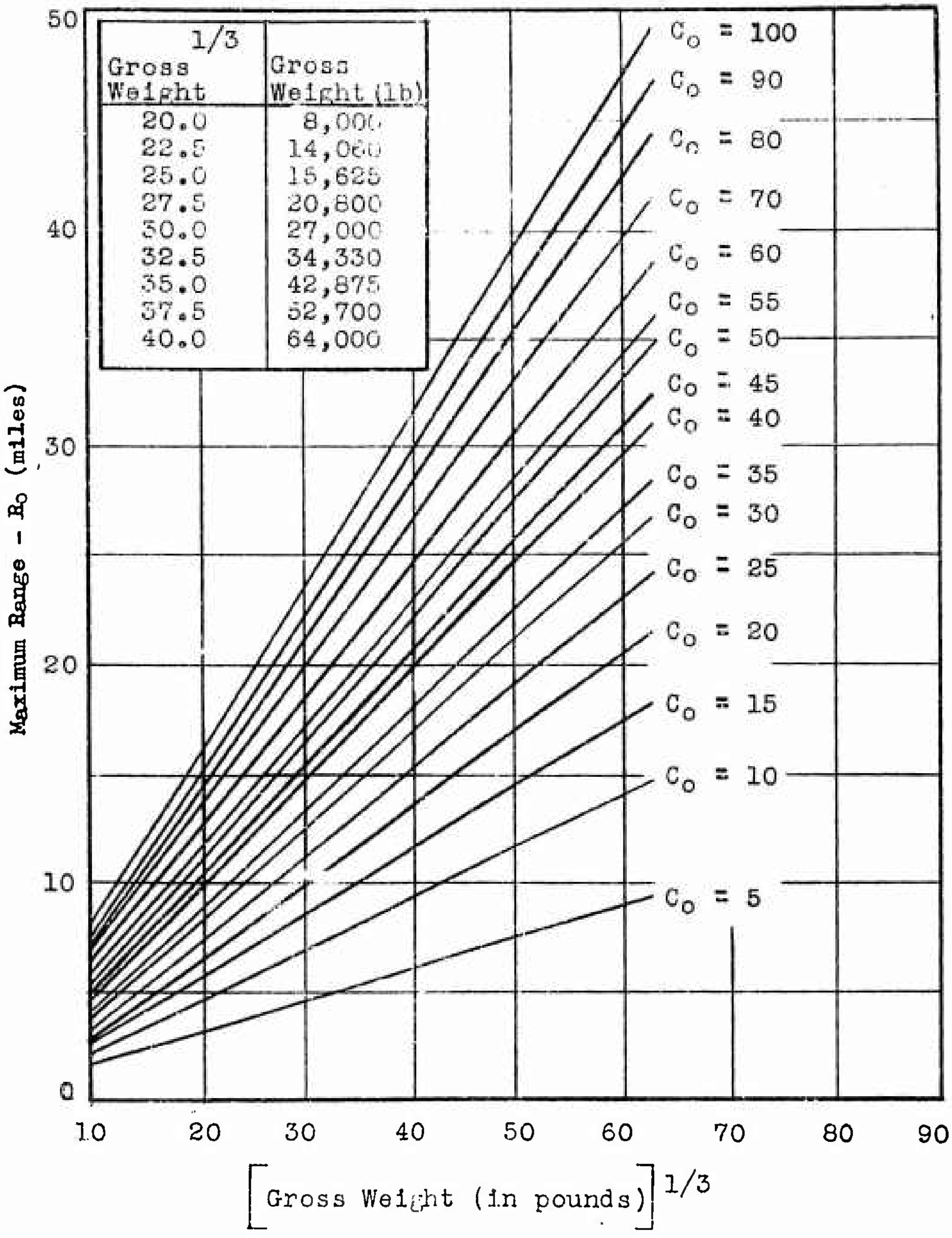

1/3 Gross Weight	Gross Weight (lb)
20.0	8,000
22.5	14,060
25.0	15,625
27.5	20,800
30.0	27,000
32.5	34,330
35.0	42,875
37.5	52,700
40.0	64,000

FIG. 3: MAXIMUM RANGE FOR BOW-ASPECT TARGETS

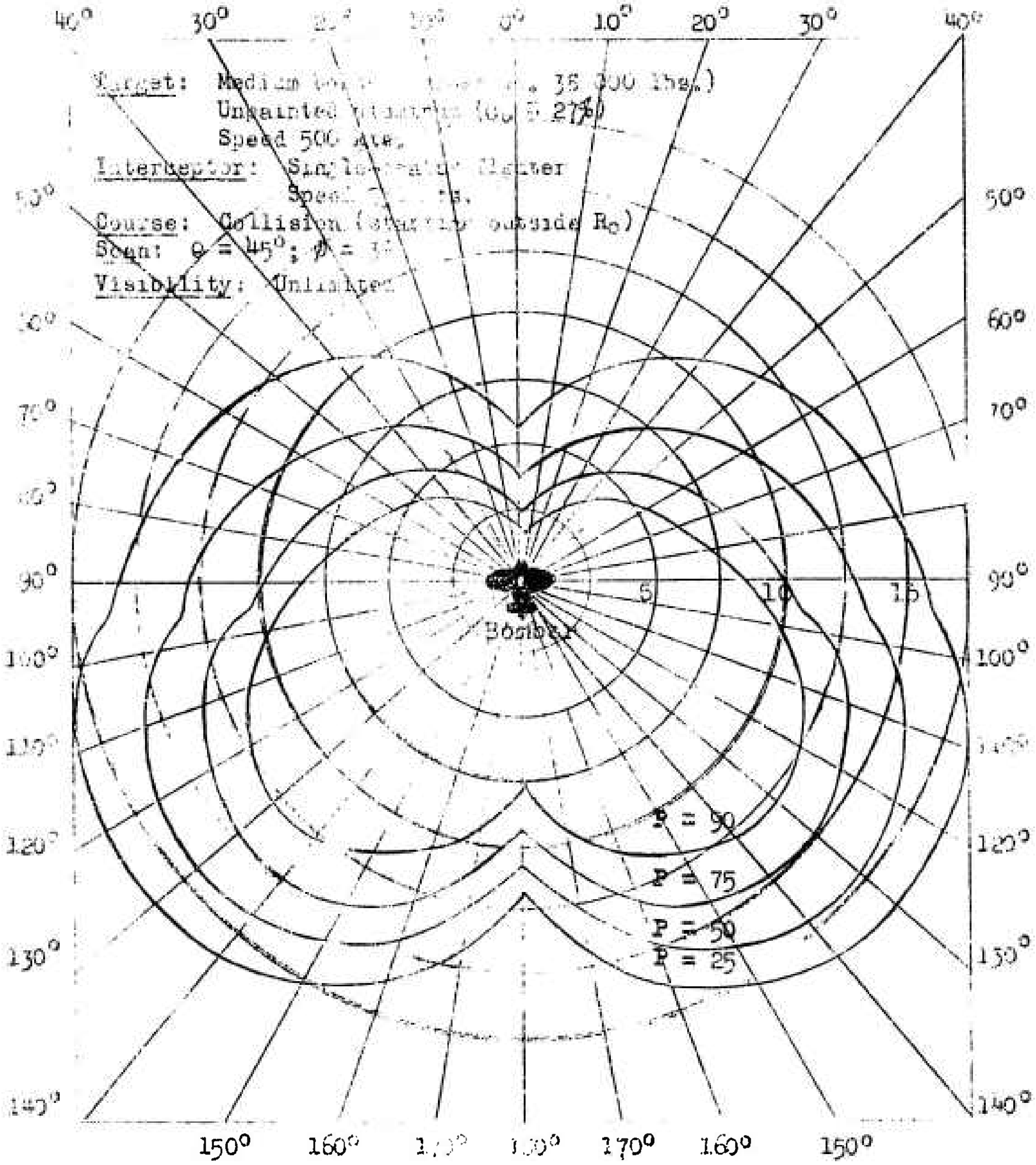

FIG. 4: RANGE [illegible] VS. ASPECT ANGLE

III. DESCRIPTION OF TESTS

[illegible] probabilities of visually de[illegible] operational conditions were per[illegible] Center, Patuxent River, Maryland [illegible] December [illegible] to September 1949. Aircraft par[illegible] were the [illegible] the F7F-3N, and the TO-1. Results [illegible] presented in [illegible].

Each trial consisted of a tracking run and a detection [illegible] tracking run provided data from which could be de[illegible] the size and shape of the detection lobe associated [illegible] target and atmosphere condition. The de[illegible] from which could be determined [illegible] the cumulative probability of detection at or [illegible] given range. Aircraft were observed on SX radar [illegible] sufficiently accurate measurements of the [illegible] between the aircraft could be made at any time.

During the tracking run, two aircraft flew at approximately equal speeds from positions abreast of one another [illegible] "start" (Figure 5) on courses diverging by 60 [illegible]. Each pilot functioned as observer, and reported to [illegible] operator of the SX radar when, after looking away from [illegible] aircraft for a moment, he could not immediately [illegible] when he looked toward it again. The operator of the [illegible] measured the separation of the two aircraft at this [illegible] to give the quantity $R_{m,120}$ (the maximum detection range under prevailing haze conditions of a target aircraft [illegible] from an aspect angle of 120 degrees off the bow).

When each aircraft was out of sight of the other, the tracking run was ended and the detection run begun (Figure 5). [illegible] aircraft were [illegible] to turn in such a manner that they [illegible] heading back toward one another from beyond maximum detection range of both aircrafts. Their speeds were so re[illegible] that the closing speed v was a predetermined quantity. [illegible] detection run each observer scanned systematically [illegible] angle (H) [illegible] 30 degrees right and left of the airline [illegible] and through angle ϕ = 3 degrees above and below the [illegible]. Each observer reported to the SX radar operator [illegible] detected the target aircraft, and the detection range [illegible] recorded.

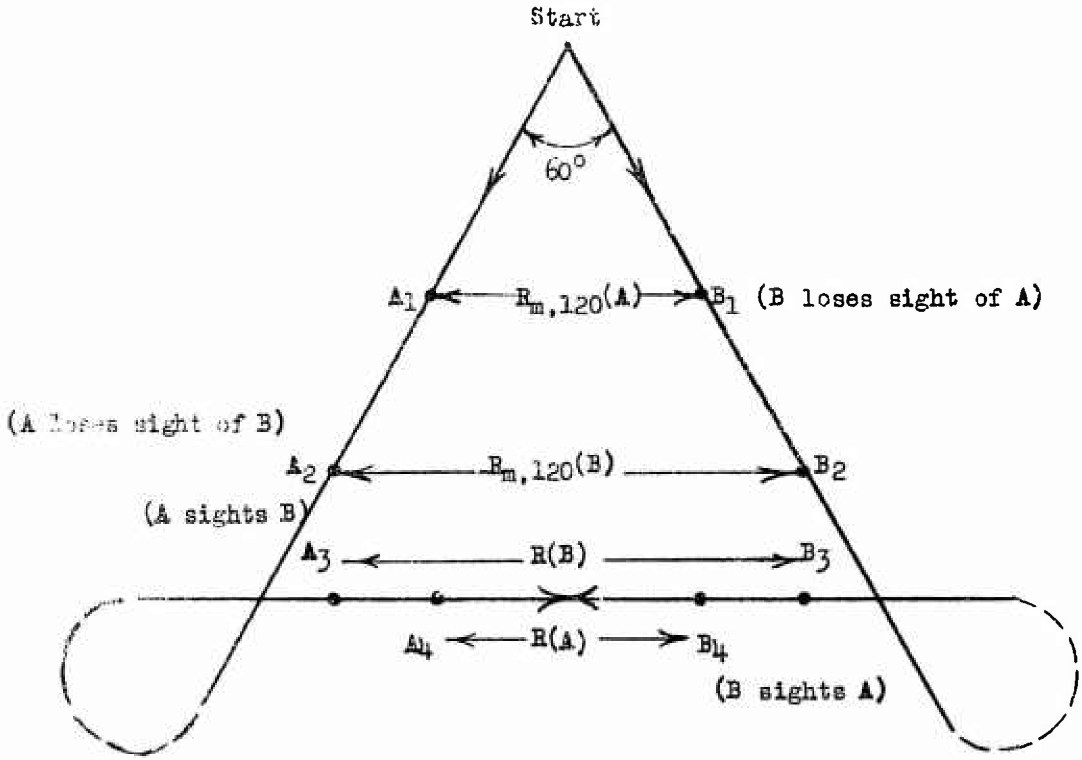

FIG. 5: DIAGRAM OF FLIGHT PATHS USED DURING TRIALS

IV. DETERMINATION OF THEORETICAL DETECTION PROBABILITIES

A. DETERMINATION OF PARAMETERS

Quantities necessary for caluclation of the theoretical probabilities of detection can be determined from the results of trials described in Section III. From these same trial results it is also possible to determine the observed probabilities of detection. (See Section V below.) The theory can be tested by comparison of these theoretical and observed probabilities.

This section of the study describes the manner of determining the quantities needed for calculating the theoretical probabilities of detection. The method of using these values to determine these probabilities is described in Section II-H.

B. DETERMINATION OF SCAN ANGLES (Θ AND Φ)

Θ is the number of degrees that the observer scans to the left or right of the expected position of the target. Φ is the number of degrees that the observer scans above or below the expected position of the target. These quantities were specified as 30 degrees for Θ and 3 degrees for Φ for all detection runs in these trials.

C. DETERMINATION OF INTRINSIC CONTRAST (C_o)

Reference (b) gives 27 percent as the intrinsic contrast against a sky background of an unpainted aluminum aircraft (TO-1) and 97 percent for the intrinsic contrast of an aircraft that was painted Navy blue. These values of C_o are used for the aircraft employed during these trials.

D. DETERMINATION OF MAXIMUM RANGE ($R_{o,\alpha}$)

$R_{o,\alpha}$ is the maximum range in the absence of haze at which the target can be detected if it is headed at an angle α off the line from observer to target. There are two methods of determining it. An "exact" method determines bow-aspect area A_o and beam-aspect area A_{90} from scale drawings

of the target aircraft and uses these figures in the following equations:

$$R_{o,o} = .1655\sqrt{(C_o-1.565)A_o} \quad \text{(equation (5), Section II)}$$

$$R_{o,\alpha} = R_{o,o}\sqrt{|\cos\alpha| + (A_o/A_{90})|\sin\alpha|}$$

This assumes that $A_{o,\alpha}$, the apparent area at aspect angle α, is the sum of the projections of the bow and beam areas.

In the "approximate" method, the maximum range at zero degrees aspect angle is assumed to be proportional to the cube root of the gross weight of the aircraft. (See Section II-I.) Then $R_{o,o}$ for any contrast can be found in Figure 3, and $R_{o,\alpha}$ can be determined from

$$R_{o,} = (\sqrt{|\cos\alpha| + 2.4|\sin\alpha|})R_{o,o}$$

Here the additional assumption that $A_o/A_{90} = 2.4$ also is made.

Calculations of $R_{o,o}$ and $R_{o,120}$ have been made using both of these methods. The results of these calculations are shown in Tables I and II. Justification of the two methods can be found in Section II and in reference (b). Weights and areas for the F8F-2 and the F7F-3N were obtained from reference (e). For the TO-1, these were determined from reference (f).

TABLE I

MAXIMUM RANGES DETERMINED BY "EXACT" METHOD

Aircraft	C_o (%)	A_o (ft^2)	A_{90} (ft^2)	$R_{o,o}$	$R_{o,120}$
F8F-2	97	62.5	147.5	12.8	20.5
F7F-3N	97	132	280	18.5	28.4
TO-1	27	53	158.6	6.1	10.7

TABLE II

MAXIMUM RANGES DETERMINED BY "APPROXIMATE" METHOD

Aircraft	C_o(%)	W(lb)	$W^{1/3}$	$R_{o,o}$	$R_{o,120}$
F8F-2	97	11,500	22.5	17	27.2
F7F-3N	97	23,900	29	22.5	36.0
TO-1	27	14,300	24.5	10	16

E. DETERMINATION OF METEOROLOGICAL VISIBILITY (V)

Meteorological visibility, the range at which large targets can be detected in the absence of haze, is not as directly determinable as the other visual detection parameters. It is a property of the atmosphere and not of the particular aircraft. Its connection with the range at which a target can be detected was given in equation (2), which may be rewritten in the following form:

$$V = (3.44\, R_{m,120})/(\log C_o - \log C_{m,120}),$$

where C_o is the intrinsic contrast in absence of haze and $C_{m,120}$ is the actual contrast of the object at a maximum range and aspect angle 120°. This latter can be obtained from $R_{m,120}$ by equations (4) and (5), which combine to give

$$C_{m,120} = (C_o - 1.565)(R_{m,120}/R_{o,120})^2$$

$R_{m,120}$, the maximum range at which a target with an aspect angle of 120 degrees can be detected, is furnished by the trial data. It was noticed that the values thus determined during each of the two periods 17 January - 8 August 1949 and 16-31 August 1949 fluctuated very little. It was therefore decided to consider the meteorological visibility constant within each period. The value of $R_{m,120}$ used to determine V for each of the two periods was the largest $R_{m,120}$ of the period. The justification for this choice is that the observers were also acting as pilots, and consequently were forced to make their observations of

maximum range with less efficiency than could have been expected if they had been acting as observers only. Disturbing factors such as the need for looking at flight instruments, the absence of reference points to facilitate relocation of the target after glancing away from it, and the irregular motion of the aircraft carrying the observer caused the observer to lose sight of the target sooner than he would under normal conditions. Consequently it was felt that the longest range at which the target was visible was close to the value that would in fact obtain under normal operating conditions.

Values of $R_{m,120}$ that were used in the computations are given in Table III. Values of V are also given in that table.

TABLE III

RANGES AND METEOROLOGICAL VISIBILITIES

Aircraft	Period	$R_{m,120}$	$C_{m,120}$		V	
			Exact	Approximate	Exact	Approximate
F8F-2	17 Jan- 8 Aug	17	65.5	37.3	147.7	60.7
F8F-2	16 Aug- 31 Aug	20.3	95.1	53.2	3535.4	116.4
F7F-3N	17 Jan- 8 Aug	18.5	42.0	40.5	76.5	73.2
TO-1	16 Aug- 31 Aug	14.3	27.0	21.9	∞	176.3

F. GROUPING OF PARAMETERS

Examination of the raw test data disclosed that the visual detection parameters would be constant over each of eight groups of trials. Each group may be characterized by the period during which the runs of the group took place, the target aircraft, and the speed with which the target aircraft closed toward the observer. The eight groups are

Data Group Number	Periods	Target Aircraft	Closing Speed
1	17 Jan - 8 Aug 1949	F8F-2	300 knots
2	17 Jan - 8 Aug 1949	F8F-2	500 knots
3	16 Aug - 31 Aug 1949	F8F-2	500 knots
4	16 Aug - 31 Aug 1949	F8F-2	700 knots
5	17 Jan - 8 Aug 1949	F7F-3N	300 knots
6	17 Jan - 8 Aug 1949	F7F-3N	500 knots
7	16 Aug - 31 Aug 1949	TO-1	500 knots
8	16 Aug - 31 Aug 1949	TO-1	700 knots

Certain trials were excluded from these groups, as explained in Appendix A. Values of the various parameters, determined for the different periods as described in this section, are summarized in Table IV. These values were used in computing the theoretical cumulative probabilities of detection. (See Section II-H and Section VI.)

TABLE IV

VISUAL DETECTION PARAMETERS DURING TRIALS

Data Group Number	Period	Aircraft	Θ°	Φ°	V (knots)	O_o(%)	$R_{o,\alpha}$ Calculation	$R_{o,o}$ (n.m.)	V (n.m.)
1	17 Jan to 8 Aug 49	F8F-2	30	3	300	97	exact	12.8	147.7
							approx	17.0	60.7
2	17 Jan to 8 Aug 49	F8F-2	30	3	500	97	exact	12.8	147.7
							approx	17.0	60.7
3	16 Aug to 31 Aug 49	F8F-2	30	3	500	97	exact	12.8	3535.4
							approx	17.0	116.4
4	16 Aug to 31 Aug 49	F8F-2	30	3	700	97	exact	12.8	3535.4
							approx	17.0	116.4
5	17 Jan to 8 Aug 49	F7F-3N	30	3	300	97	exact	18.5	76.5
							approx	22.5	73.2
6	17 Jan to 8 Aug 49	F7F-3N	30	3	500	97	exact	18.5	76.5
							approx	22.5	73.2
7	16 Aug to 31 Aug 49	TO-1	30	3	500	27	exact	6.1	∞
							approx	10.0	176.3
8	16 Aug to 31 Aug 49	TO-1	30	3	700	27	exact	6.1	∞
							approx	10.0	176.3

V. DETERMINATION OF OBSERVED CUMULATIVE DETECTION PROBABILITIES

Section IV described the method of obtaining theoretical probabilities of detection from the trial results. The present section gives means of calculating the cumulative probabilities of detection that actually were observed in the trials. Section VI will compare the two sets of probabilities.

Observed cumulative probabilities of detection for each group of trials (Section IV-F) are determined from the detection ranges that occur during the detection runs (Section III). The n runs of the group are arranged and numbered in decreasing order of the detection ranges observed on each run, so that

$$R_1 \geqslant R_2 \geqslant R_3 \geqslant \cdots \geqslant R_i \geqslant \cdots \geqslant R_n,$$

where R_i is the detection range observed on the ith run. Failures to detect are recorded at range zero.

Then the observed cumulative probability of visual detection associated with the ith run is i/n at range R_i.

VI. COMPARISON OF OBSERVED AND THEORETICAL PROBABILITIES OF DETECTION

The validity of the theory of visual detection that was outlined in Section II can be assessed by comparing the cumulative probabilities of detection that were observed during the Patuxent trials with the corresponding probabilities that were determined by the theory.

To make the comparison, an 80-percent cumulative frequency belt was drawn around the curve of theoretical probability that had been determined from each group. These belts are defined as those within which 80 percent of the observations can be expected to lie. They were determined with the assistance of the theory of binomial distributions, as described in Appendix B. A sample curve with its belt is shown in Figure 6.

After these belts were drawn, the observed probabilities of detection for each group of trials were plotted on the corresponding graphs of the theoretical probabilities and 80-percent belts. For each graph, a count was made of the number of observed cumulative probabilities plotted above the 80-percent belt, within the belt, and below the belt. Failures were counted as occurring below the belt.

If the theory adequately described the detection process, 10 percent of the observed probabilities should lie above the theoretical 80-percent belts, and 10 percent of them should lie below the 80-percent belts. The actual percentages in each belt are shown in Table V.

TABLE V

PERCENTAGES IN FREQUENCY BELTS

Method	Percentage of Observed Probabilities				
	Above 80% belt	Within 80% belt		Below 80% belt	Total
		upper half	lower half		
Exact	19	40	28	13	100
	59	68	41		
Approximate	44	35	20	1	100
	79	55	21		

Table V demonstrates the close agreement between the results of the exact theoretical method and the observed test results. Agreement is not as close for the results of the approximate theoretical method. It was not expected, of course, that it would be. It is unlikely that the approximate method will be used if the required information (size of the aircraft (See Section IV-D)) is available. In many actual cases, unfortunately, the size and shape of the target aircraft will not be known. Then the approximate method, which utilizes the gross weight of the aircraft will be useful.

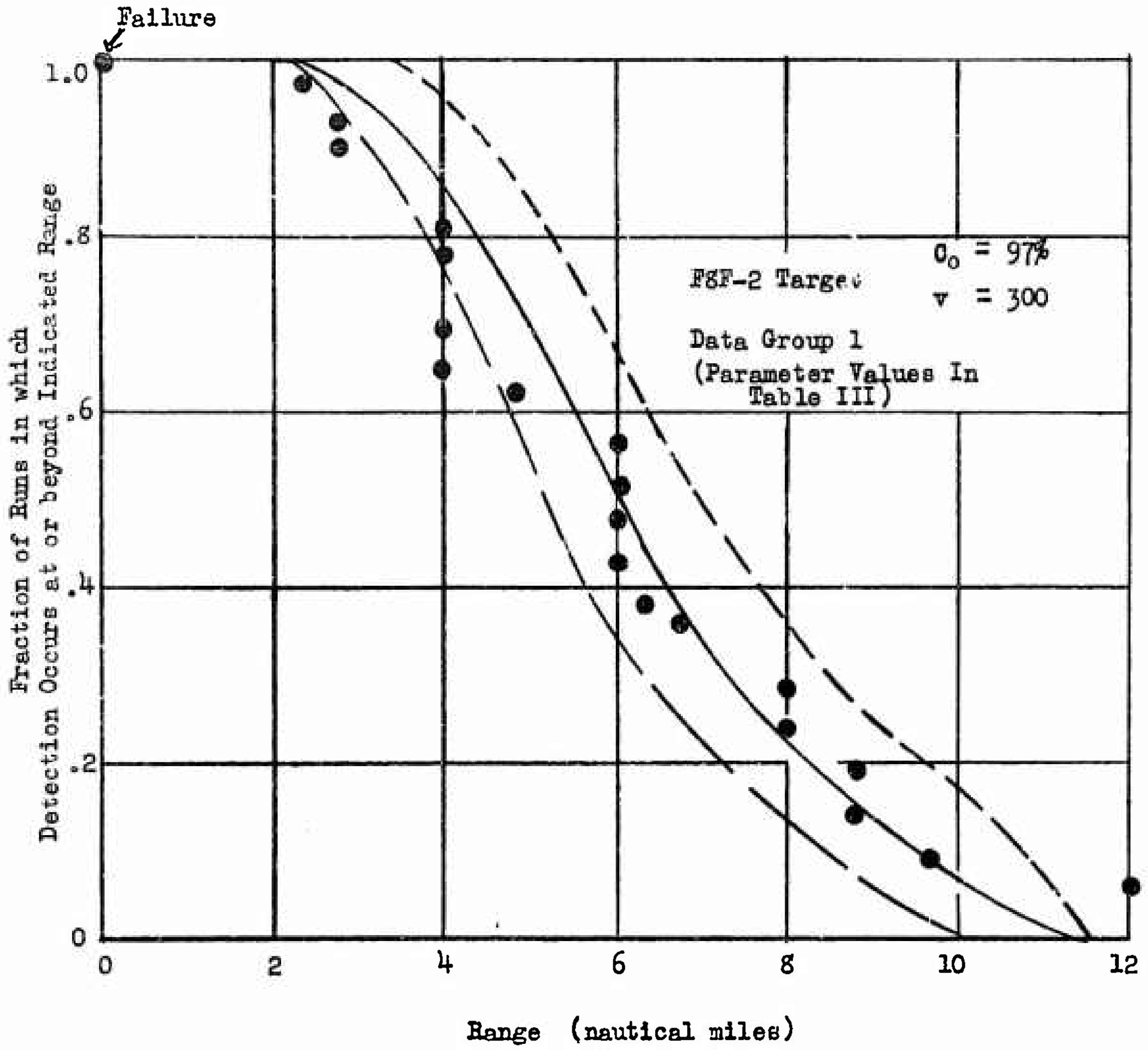

FIG. 6: COMPARISON OF THEORETICAL AND EXPERIMENTAL CUMULATIVE PROBABILITIES OF DETECTION

VII. CONCLUSIONS

On the basis of the trial results, it can be concluded that the visual detection theory presented in reference (b) satisfactorily predicts cumulative probabilities of detection when the so-called "exact" method is used. In this method the maximum range in absence of haze is determined from the aspect area of the target. However, when this range is determined from considerations of the weight of the airplane, the so-called "approximate" method, agreement between theory and experiment is not as satisfactory.

Examination of the relatively small number of trials analyzed in this study reveals that the "exact" method gives slightly smaller detection probabilities than are observed in practice. This conservatism is not extreme, and may be accounted for by two conditions:

(1) Specular reflection aids detection, and is not considered in the theory. Although detections that obviously were facilitated by sunflash have been excluded from the computations, it is possible that some detections might have been assisted by sun reflections that were not recognizable as such. This would give a large detection range and so increase the observed detection probability.

(2) Since there were no reference points, it was difficult to enforce the scanning procedure. A tendency for observers to scan the center of the field more thoroughly than the edges was noted on the data sheets. This would reduce the horizontal scanning angle, which would tend to produce detections at greater ranges than those predicted by a theory using the erroneous larger horizontal scanning angle.

Submitted by:

J.H. ENGEL
Operations Evaluation Group

Approved by:

D.L. BROOKS
Deputy Director
Operations Evaluation Group

APPENDIX A

TRIAL DATA AND REASONS FOR OMISSION OF CERTAIN TRIALS

Tables A-1 to A-5 present the data from trials conducted at the Naval Air Test Center, Patuxent River, Maryland, from 17 December 1948 to 20 September 1949. These trials were conducted to determine the probabilities of visually detecting aircraft under operational conditions, and from the basic data from which the worth of the visual detection theory was assessed. Certain of the data listed in these tables were not used in making this analysis. Enumeration of the rejected data and reasons for their omission follow.

Data taken on 17 December 1948 and 1 and 6 September 1949 were not used. On 17 December 1948 no tracking turns were made, and no experimental determination of meteorological visibility was possible. Consequently there existed no basis for making a comparison with the results obtained on the detection runs.

On 1 and 6 September 1949, seven sets of observations of a P2B-1S were made. Because this aircraft was painted black on the underside and was of unpainted aluminum above, it was not possible to determine a logical value of C_0 for use in calculating the theoretical probabilities of detection. Calculations with $C_0 = 97$ percent have been made. These give a good fit of observed and theoretical probabilities of detection (all points fall within the 80-percent frequency belts) and also give close agreement between observed and theoretical haze-free maximum ranges. However, the results are not considered significant and have not been used.

In each of the periods, 17 January - 8 August 1949, and 16 - 31 August 1949, the observed values of $R_{m,120}$ for each aircraft fluctuated in general between fairly narrow limits independent of the closing speed. It was decided therefore to consider that the meteorological visibility was constant within each period. On this basis, the results of the runs made on 17 May have not been included in this analysis, since for both participating aircraft the observed values of $R_{m,120}$ were all considerably lower than the values generally observed on the other runs made during the same period.

Results of tracking run 4(TO-1) on 17 August 1949 and tracking runs 10 and 12 on 31 August 1949 are attributed to sunflash and hence are not included since they represent maximum visual ranges obtained under atypical conditions.

The results of detection runs made on 17 May have not been included, since, as has been pointed out earlier, they were conducted under different visibility conditions than the other runs in that period, and there were not enough of these runs to warrant their separate analysis.

During the detection runs made on 17, 18 May, 29 July and 3 August, instead of being vectored directly toward each other (as was the case in all other detection runs) the participating aircraft were vectored on anti-parallel courses passing some small distance (called flight-path separation) abeam of one another. Although, under such conditions, detections would ordinarily occur at slightly smaller ranges than on head-on detection runs, the data from these runs have been handled in the same manner as the data obtained from the other detection runs (except runs on 17 May which have already been excluded from consideration for reasons discussed earlier). The inclusion or exclusion of these runs should not materially affect any of the results since in most cases the flight-path separation was quite small.

Detection runs 5 and 6 on 23 August have not been included. On these runs detections were reported as having occurred at an unspecified range and outside the field of scan. Since the manner of handling such data is highly questionable, these results have been excluded from further consideration.

TABLE A-1
RESUME OF RUNS 300 KNOTS CLOSING SPEED
10,000 FEET ALTITUDE

50° Scan

Run No.	Date	Flight Path Separation	Sighting on F7F-1N with Drop Tank Max. Vis.	Intercept	Sighting on F8F-[illegible] Max. Vis.		Remarks
1	17 Dec 48	---	----	9.0	----	5.0	Accurate clock code information.
2		---	----	8.0	----	5.0	Minimum scan angle.
3		---	----	9.0	----	8.0	
4		---	----	10.0	----	5.0	
5		---	14.0	5.0	12.0	4.0	Minimum scan angle. (etc.)
6	17 Jan 49	---	18.0	10.0	12.0	4.0	Clock code information had direct bearing on intercept range.
7		---	17.0	6.0	15.0	12.0	
8		---	12.5	6.0	12.0	6.0	
9		---	14.0	no run	10.5	no run	
10	18 Jan 49	---	9.0	14.0	6.0	3.0	3,000 ft. altitude due to weather.
11		---	14.0	3.0	11.0	6.0	
12		---	13.0	12.0	11.0	4.0	Minimum scan angle. Poor clock code information.
13	27 Jan 49	---	14.0	7.0	12.5	missed	6,000 ft. altitude.
14		---	15.0	11.0	15.0	7.0	Minimum scan angle.
15		---	14.5	13.0	13.8	8.0	
16	13 May 49	---	16.0	9.0	14.0	6.0	Commenced controlled scan limits and scan procedures. All intercepts directly on 12:00 clock code. Tends to discourage scanning. Suggest flight path separation to enforce scanning.
17		---	15.0	8.0	10.0	9.0	
18		---	15.0	6.0	14.0	9.0	
19		---	11.5	5.5	11.0	6.5	
20		---	16.0	9.5	11.0	9.5	
21		---	12.5	11.0	16.0	8.0	

TABLE A-1 (CONTINUED)

Run No.	Date	Flight Path Separation	Sighting on F7F-3N with Drop Tank Max. Vis.	Sighting on F7F-3N with Drop Tank Intercept	Sighting on F8F-2 Max. Vis.	Sighting on F8F-2 Intercept	Remarks
22	17 May 49	3.0	7.0	Miss	8.0	3.6	Flight path separation of over 1.5 miles appears to cause very erratic results. This limit will be utilized in later runs to enforce scanning. Misses here are not believed indicative.
23		1.5	8.5	5.9	7.5	5.7	
24		3.0	8.5	Miss	7.0	5.0	
25		2.5	7.5	Miss	7.0	Miss	
26		2.0	9.0	Miss	9.0	4.0	
27		1.0	9.0	4.6	7.0	3.2	
28		3.0	7.5	3.1	7.0	4.0	
29	18 May 49	.50	18.0	7.0	14.5	6.0	Flight terminated due to radar difficulty.
30	29 Jul 49	1.0	12.0	7.0	11.0	5.0	
31		2.5	15.0	12.0	12.0	3.0	
32		0.0	16.0	7.0	9.0	4.0	
33		1.0	16.0	4.0	9.5	2.5	

TABLE A-2

[illegible]

Run No.	Date	[illegible] Separation	Signals with Drop Tan. Max. Vis.	Signals with Drop Tan. Intercept	Signals [illegible] Max. Vis.	Signals [illegible] Intercept	[illegible]
1	17 Dec 48	-----	-----	4.5	-----	3.5	
2		-----	-----	10.0	-----	7.0	
3		-----	-----	12.0	-----	Miss	
4	27 Jan 49	-----	14.0	13.0	12.5	3.5	
5		-----	15.0	4.5	15.0	8.0	
6		-----	None	4.0	None	10.0	
7	3 Aug 49	2.5	17.5	4.0	14.0	[illegible]	Using controlled [illegible] angle [illegible] procedure.
8		3.0	None	7.0	None	[illegible]	
9		4.0	16.0	6.0	14.0	[illegible]	
10		1.5	14.0	7.0	13.0	8.0	
11		1.5	16.0	6.0	12.0	7.0	
12		1.0	12.0	7.0	14.0	7.0	
13	4 Aug 49	None	16.0	4.0	5.0	5.0	Many thunder storms cause erratic results.
14		-----	16.0	6.0	12.0	1.0	
15		-----	18.0	11.0	13.0	11.0	
16		-----	15.0	3.0	8.0	4.0	
17		-----	12.0	7.0	9.0	8.0	
18		-----	10.5	6.0	12.0	5.0	
19		-----	16.0	None	8.0	None	
20	8 Aug 49	-----	16.0	11.0	11.0	4.0	
21		-----	14.0	7.0	16.0	3.0	
22		-----	16.0	9.0	13.0	5.0	
23		-----	17.0	13.0	12.0	7.0	
24		-----	17.0	8.0	11.0	5.5	
25		-----	16.0	6.5	9.0	8.0	

TABLE A-3
RESUME OF RUNS 500 KNOTS CLOSING SPEED
30,000 FEET ALTITUDE

60° Scan Angle

Run No.	Date	Sighting on F8F-2 (tame)		Sighting on TO-1 (unalerted)		Random Intercepts
		Max. Vis.	Intercept	Max. Vis.	Intercept	Remarks
1	16 Aug 49	19.0	4.5	12.0	4.0	
2		16.0	3.5	12.0	1.0	
3	17 Aug 49	18.0	5.0	14.0	3.0	
4		20.0	8.0	*16.0	2.0	
5		16.0	7.5	12.0	3.0	
6		14.0	7.0	7.0	4.0	
7		16.0	8.0	11.0	5.0	
8		None	8.0	None	0.5	
9	19 Aug 49	16.0	2.5	10.0	5.0	
10		19.0	8.0	13.0	1.5	
11		None	8.0	None	4.0	

* Extreme range due to sunflash

TABLE A-4

[illegible]

30,000 FEET ALTITUDE

Run No.	Date	Sighting on F8F-2 (blue) Max. Vis.	Intercept	Sighting on D-1 [illegible] Max. Vis.	Intercept	Remarks
1	22 Aug 49	19.0	None	12.0	None	
2		None	8.5	None	1.5	
3		15.0	5.0	11.0	3.0	
4	23 Aug 49	17.0	8.0	13.0	1.5	
5		14.0	Out of Scan	10.0	Out of Scan	
6		None	Out of Scan	None	Out of Scan	
7	30 Aug 49	16.0	6.0	6.0	1.5	
8		15.0	5.0	6.0	1.5	
9		12.0	3.0	7.0	2.0	
10		16.0	1.5	**14.0	3.0	
11		18.0	8.5	8.0	2.0	
12		19.0	3.5	**16.0	3.5	
13	31 Aug 49	18.0	7.0	10.0	1.5	
14		14.0	11.0	None	1.5	

** Extreme ranges due to sunflash

TABLE A-5

RESUME OF RUNS 500 KNOTS CLOSING SPEED
20,000 FEET ALTITUDE

60° Scan Angle — Head-on Intercepts

Run No.	Date	Sighting on F2B-1S Max. Vis.	Sighting on F2B-1S Intercept	Sighting on [illegible] Max. Vis.	Sighting on [illegible] Intercept	Remarks
1	1 Sep 49	36.0	40.0 (On Contrails)	None	None	
2	6 Sep 49	35.0	16.0	"	"	
3		37.0	22.0	"	"	
4		32.0	11.0	"	"	
5		35.0	18.0	"	"	
6		33.0	24.0	"	"	
7		37.0	24.0	"	"	

[illegible]PENDIX

[illegible] FREQUENCY BELTS

[illegible] Eisenhart, [illegible] F [illegible]

[illegible] cumulative [illegible] of signal detection observed during those [illegible] to determine whether or not there appears to [illegible] between the observations and the theory. [illegible], the theory of [illegible] distributions ([illegible] reference (a), footnote page 336, and [illegible])) has been utilized, as follows:

[illegible] frequency belts were placed [illegible] curve. If P(R) [illegible] the theoretical [illegible] probability [illegible] detected at or beyond [illegible] R, [illegible] reference (a) [illegible] P = P(R), [illegible] applies (ob-[illegible]) [illegible] upper and lower [illegible](R) [illegible] L(R) [illegible]-percent belt [illegible] R. P[illegible] upper and lower limits on the [illegible]

[illegible] a [illegible], [illegible], 50 per-[illegible] belts, 10 percent [illegible], [illegible] percent [illegible]

[illegible] of an event ([illegible] on a given trial is independent of results of other trials), then P(x,n), the probability of exactly [illegible] $\leqslant$ [illegible] $\leqslant n$) [illegible] event in n trials, is (by [illegible])

[illegible] At [illegible], P([illegible] $\leqslant x \leqslant$ [illegible], n), [illegible]);

the probability of not less than a nor more than b occurrences of the event on n trials ($0 \leqslant a \leqslant b \leqslant n$) is

$$\sum_{i=a}^{b} P(i,n) = \sum_{i=a}^{b} \frac{n!}{i!\,(n-i)!}\, p^{i}\,(1-p)^{n-i}$$

The limits of the 80-percent frequency belt for a given probability p, and a given number of trials, n, are obtained by choosing values of a and b located as symmetrically as possible about np (the expected number of occurrences) in such a manner as to yield a value for $P(a \leqslant x \leqslant b, n)$ as close to .80 as possible.

It is by this procedure (or approximations to it, in which the incomplete Beta Function is used) that the curves in Figure 10.4 of reference (a) have been obtained.

APPENDIX C

COMBINING STATISTICS FROM RUNS MADE UNDER DIFFERENT CONDITIONS

One of the desirable characteristics of a useful visual detection theory is the ability of the theory to combine the results of runs made under different conditions. In this appendix a method is described for combining results in testing any detection theory that predicts cumulative probability of detection by any given range as a function of the various conditions under which the detection was made, no specific reference to the exact nature of the theory need be made. With such a procedure for combining data from runs made under different conditions, the operational validation of a given theory may be made more quickly and economically than might be possible, if it were necessary to run large numbers of carefully controlled trials and vary the pertinent parameters one by one.

Let P_i be the <u>theoretical</u> cumulative probability of detection obtained during run i, and number the runs in such a manner that

$$P_i \leqslant P_j \quad \text{whenever} \quad i < j \qquad (1 \leqslant i \leqslant n)$$

Let

$$d_i \begin{cases} = 1 \text{ if a detection occurred by the end of run i} \\ = 0 \text{ if no detection occurred during run i} \end{cases}$$

Then the <u>observed</u> cumulative probability of detection corresponding to the <u>theoretical</u> cumulative probability of detection

$$P_k \text{ is } \frac{\sum_{i=1}^{k} d_i}{k}$$

A graph of observed probability of detection (P_{obs}) versus theoretical probability of detection (P_{th}) is shown in Figure C-1 together with the [illegible]-percent frequency belts for 131 runs.

A similar graph in which the scale distance from the origin is proportional to -log(1 - P) along each axis (the graph is [illegible] paper turned upside down with the axes suitably labeled) is shown in Figure C-2.

On both graphs the 45° lines drawn up from the origin represent the line along which all observed probabilities in perfect agreement with the corresponding theoretical probabilities would be plotted.

Both graphs show that for small and intermediary probabilities, the theory is slightly pessimistic, i.e., yields slightly smaller results than are observed in practice, and that for high probabilities the theory is slightly optimistic.

The graph shown in Figure C-2 has an additional property which can be useful. A straight line through the origin which provides a good fit to the plotted observations shown has a slope which can be thought of as a correction factor to be applied to T, the time between successive glimpses stated in reference (a) to be 1.63 seconds. Since the slope of such a line is

$$\frac{-\log(1 - P_{obs})}{-\log(1 - P_{th})}$$

and since

$$P = 1 - \exp\left[(1/T)\int \log(1 - p)\,dt\right]$$

it follows that

$$-\log(1 - P) = (1/T)\int -\log(1 - p)\,dt,$$

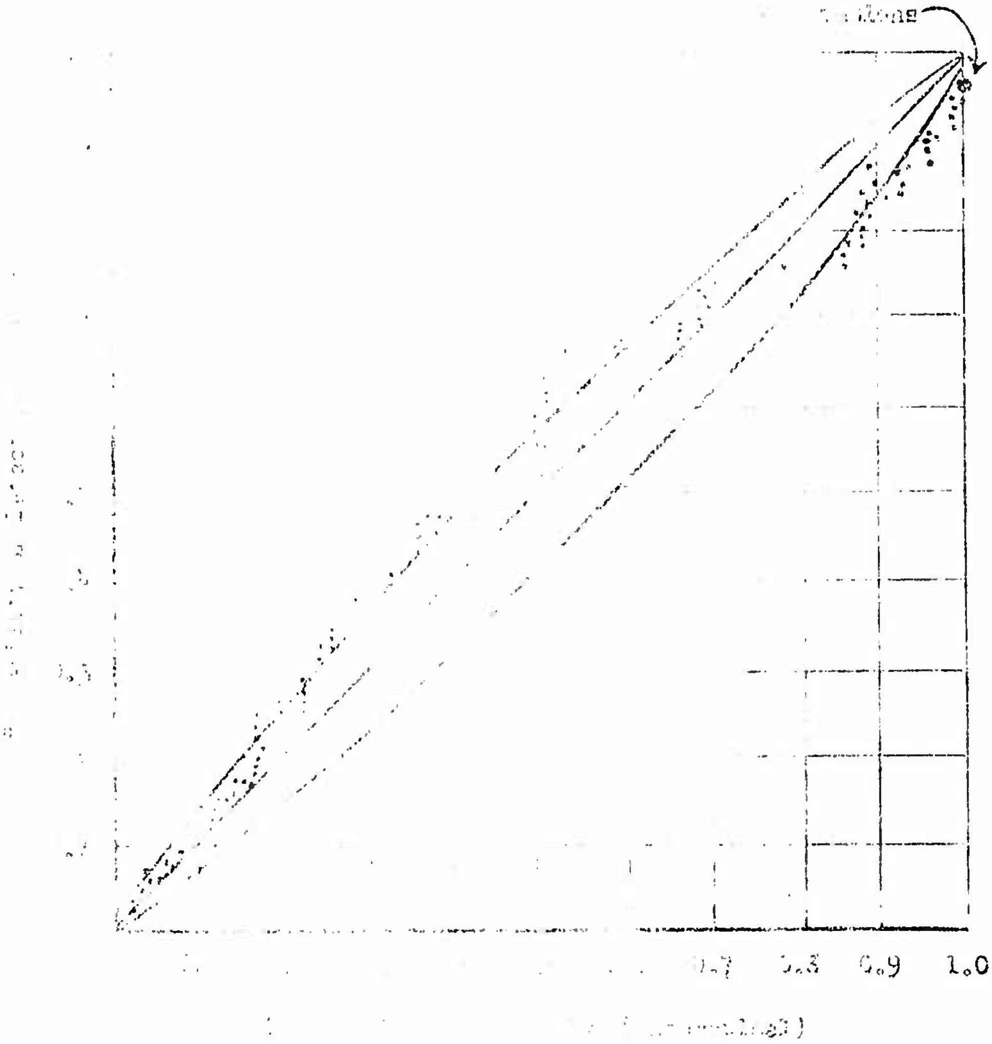

0.7
0.8
0.9
1.0

[illegible]

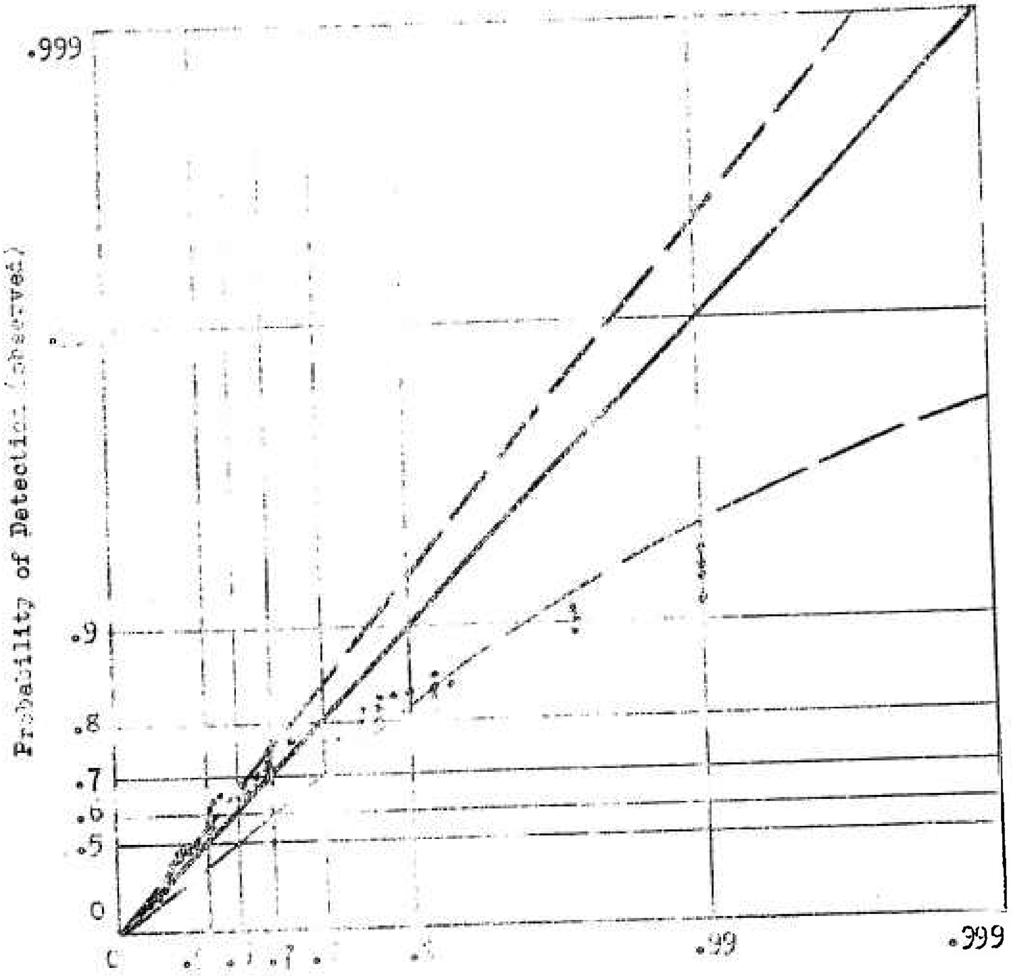

Probability of Detection (Theoretical)

FIG. C-2: COMPARISON OF OBSERVED AND THEORETICAL PROBABILITIES

[illegible]

[illegible] that

[illegible] to [illegible] slope [illegible] type [illegible]

[illegible]

[illegible] all other [illegible] the right [illegible] T, the time [illegible] a value [illegible] points [illegible] and the uncer- [illegible], no [illegible]. It is [illegible] which [illegible] indicate a [illegible] of T, the [illegible]